



Hounsfield unit values of liver pathologies in unenhanced post-mortem computed tomography

Carmen Tisch¹ · Eva Brencicova¹ · Nicole Schwendener¹ · Paolo Lombardo^{1,2} · Christian Jackowski¹ · Wolf-Dieter Zech¹

Received: 19 September 2018 / Accepted: 1 February 2019
© Springer-Verlag GmbH Germany, part of Springer Nature 2019

Abstract

Background The goal of this study was to evaluate if unenhanced PMCT HU values of liver pathologies differ from post-mortem HU values of non-pathologic liver tissue.

Methods Liver HU values were measured in five liver segments in PMCT unenhanced datasets of 214 forensic cases (124 male, 90 female, mean age 54.3 years). Liver HU values were compared with corresponding histologic liver findings. HU values of non-pathologic livers were compared to HU values of liver pathologies.

Results A total of 64 non-pathologic livers (mean HU 58.32, SD 8.91) were assessed. Histologic diagnosed liver pathologies were as follows: steatosis ($n = 121$ (grade I $n = 61$, grade II $n = 37$, grade III $n = 23$)), fibrosis ($n = 10$), and cirrhosis ($n = 19$). HU values of the livers exhibiting severe steatosis (mean HU 32.44, SD 13.76), fibrosis (mean HU 44.7, SD 16.31), and cirrhosis (mean HU 50.59, SD 9.42) significantly differed to HU values of non-pathologic livers at ANOVA testing.

Conclusion PMCT unenhanced liver HU value measurements may be used as an additional method to detect unspecific liver-pathology. Values below 30 HU may specifically indicate severe steatosis.

Keywords Unenhanced post-mortem computed tomography · Liver · Hounsfield unit · Steatosis · Fibrosis · Cirrhosis

Introduction

In recent years, post-mortem computed tomography (PMCT) has been established as a useful tool in post-mortem examinations. While unenhanced PMCT is particularly useful for visualization of foreign bodies, bone fractures, gas, and fluid accumulations, it is rather insufficient for soft tissue analysis [1–3]. In clinical CT images as well as PMCT images, a basic tissue analysis can be accomplished by measurements of Hounsfield units (HU) of tissues and organs [6–10]. On the Hounsfield scale, the radiodensity of distilled water at standard pressure and temperature is defined as zero HU, and the

radiodensity of air is defined as -1000 HU [11]. In the living, different tissues and fluid media possess characteristic HU magnitudes and ranges [4, 5, 12–14]. The non-pathologic liver shows in vivo HU values between 50 and 65 [15]. It is known that liver pathology may alter in vivo liver radiodensity which translates into altered HU values in CT scans. Liver steatosis, for instance, decreases liver radiodensity and thereby liver HU values [15–19]. It appears logical to assume that liver pathology such as liver steatosis can also be assessed in post-mortem computed tomography images by HU measurements. However, PMCT is vastly different from clinical CT due to various post-mortem phenomena, such as putrefaction, biochemical degradation and diffusion processes [3, 20]. These phenomena may alter radiodensity of post-mortem liver tissue even in a short post-mortem interval of a few days. Thus, known in vivo HU liver values cannot be simply applied to PMCT applications. So far, HU values of non-pathologic livers and liver pathologies have not been analyzed systematically in PMCT. Hence, post-mortem HU values of non-pathologic livers and liver pathologies (PMI) are not clarified. Therefore, the goal of this study was to assess HU values of livers in PMCT and to evaluate if post-mortem HU values of

✉ Wolf-Dieter Zech
wolf-dieter.zech@irm.unibe.ch

¹ Institute of Forensic Medicine, University of Bern, Buehlstrasse 20, 3012 Bern, Switzerland

² Department of Diagnostic, Interventional and Pediatric Radiology, Inselspital, University Hospital, University of Bern, Freiburgstrasse 8, CH-3010 Bern, Switzerland

liver pathologies differ to post-mortem HU values of non-pathologic liver tissue.

Methods

Study population

A total of $n = 300$ forensic cases were screened retrospectively. All cases underwent post-mortem computed tomography prior to forensic autopsy during the years 2013 and 2014 at the authors host forensic institution. Of the 300 cases, those with either age less than 18 years, traumatic liver damage as well as autoptical (based on autopsy reports) or radiologic signs of advanced liver putrefaction (grade II (moderate emphysema) or grade III (extensive emphysema) of gaseous amounts in liver parenchyma and vessels according to Egger et al. [21]) were excluded. Moreover, cases with liver tumors ($n = 3$) or liver cysts ($n = 4$) as well as cases exhibiting exsanguination (bloodless livers, $n = 6$) were omitted from the study because case numbers were too low to allow for statistical analysis. Thus, of a total of $n = 300$ screened cases, $n = 86$ cases were excluded. Causes of death in the remaining 214 cases that were analyzed for liver HU values were: sudden cardiac death ($n = 122$), myocardial infarction ($n = 34$), intoxication ($n = 28$), pulmonary embolism ($n = 12$), suffocation ($n = 6$), asphyxia ($n = 5$), hanging ($n = 4$), and metabolic derailment ($n = 3$).

PMCT settings

A Somatom Definition AS 64 (Siemens, Forchheim, Germany) CT scanner was used with the following settings: beam energy 130 kV; collimation 64×0.6 mm; rotation time 500 ms; image reconstruction was performed with a slice thickness of 1.0 mm and an increment of 0.7 mm using a soft tissue kernel (I31 f); the field of view was adapted to the size of the object. For whole-body CT scanning, corpses in body bags were placed on the CT table in supine position. The arms of corpses were left resting beside the torso. All CT scans were performed native without usage of contrast agent. Use of the imaging data was approved by the local ethics committee.

Autopsy and histology

Forensic autopsies were mandated by the local authorities. Autopsies were performed by board certified forensic pathologists immediately after PMCT. External and internal examination of corpses was performed according to the Recommendation of the Committee of Ministers to Member States of Europe on the harmonization of medico-legal autopsy rules [22]. All three body cavities were opened and all organs were dissected. The liver was dissected into 1-cm thick

slices. Macroscopic appearance of the livers and visible pathologic liver findings were noted in autopsy reports. Tissue specimens for histologic analysis were obtained from each liver from the right and left liver lobe. In those cases where focal liver lesions were present, additional specimens of those lesions were obtained. Standard histologic stainings (hematoxylin and eosin (H&E) and chromotrope aniline blue (CAB, special staining used to highlight fibrosis)) were conducted in each case. Histologic diagnosis was conducted by board certified forensic pathologists and noted in the autopsy report. In those cases where liver steatosis was diagnosed, a grading system based on numbers of hepatocytes with fatty vacuoles in % was used according to Brunt [23]: grade 0, < 5% non-pathologic; grade I, 5–33% slight steatosis; grade II, 34–66% moderate steatosis; grade III, > 66% severe steatosis.

PMCT HU measurements

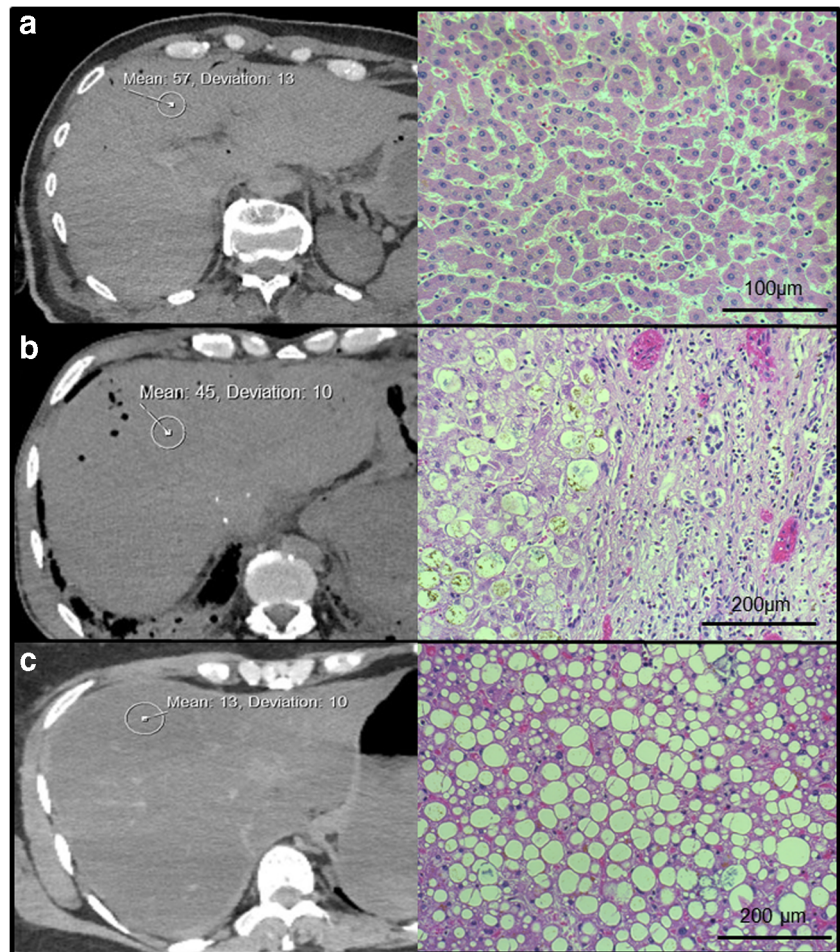
The livers in whole-body PMCT datasets were analyzed in axial view in a commercially available PACS (Sectra Workstation IDS7 Version 17.1.16.3569, ©2015 Sectra AB Linköping/Sweden). Regions of interest (ROI) were placed in the right and left liver lobe in five liver segments on different axial slices (Fig. 1). The size of the ROIs was approximately 1.5 cm in diameter. In cases where focal liver lesions were visible, those lesions were measured separately. ROIs were deliberately not placed in visible larger liver vessels. Measurements were conducted blinded to autopsy results by a medical student (observer one) who was trained in reading and HU measuring PMCT liver images by a forensic pathologist with 10 years of experience in PMCT imaging. Arithmetic means and standard deviations of liver HU measurements were calculated for each single liver. Each mean liver HU value was assigned its corresponding histological diagnosis according to autopsy reports. Focal liver lesions were separately assigned their corresponding histological diagnosis and mean HU values. Liver pathologies found within the study group were divided into individual groups such as steatosis, and cirrhosis.

Statistical analysis

SPSS® (Version 23.0) was used to perform statistical analysis. A series of one-way ANOVAs with post-hoc analysis was conducted to evaluate significant differences of HU values of groups with liver hyperemia as well as structural liver pathology and non-pathologic livers. Bonferroni correction was applied: significant p values < 0.05.

Intra-observer error of HU liver measurements was estimated using a random selection of 20 cases of the study group. After a time lapse of 2 months, liver HU values were re-measured in the same PMCT datasets by the same observer (observer one). Inter-observer error of liver HU measurements

Fig. 1 HU measurements in PMCT liver images HU values were measured in PMCT livers and assigned a corresponding histological diagnosis. The figure exemplarily shows HU values of non-pathologic liver (**a**), liver cirrhosis (**b**), and severe liver steatosis (**c**). Histological images shown were all stained with H&E



was estimated using randomly selected PMCT images of 20 corpses within the study group. Two observers (observer one and observer two (radiographer with 7 years of experience in PMCT)) independently measured HU liver values of the same PMCT datasets. For assessment of intra-observer error and inter-observer error the difference between two HU measurement series (observer one vs observer one; observer one vs observer two) were calculated. A *t* test for paired samples was applied to assess the significance of the differences between measurement series. *p* values < 0.05 were considered to be significant.

Results

A total of $n = 214$ cases (124 male, 90 female, mean age 54.3 years) were measured for their liver HU values. Measurement of five liver segments was possible in each case. According to histologic diagnoses, the following groups were determined: non-pathologic livers $n = 64$; liver cirrhosis $n = 19$; liver fibrosis $n = 10$; liver steatosis $n = 121$ (grade I (slight steatosis) $n = 61$; grade II (moderate steatosis) $n = 37$; grade III

(severe steatosis) $n = 23$). Table 1 provides information about sex, mean age, and mean post-mortem interval (PMI, time from death to CT scan) for each group. Table 2 gives the mean HU of non-pathologic livers and groups with structural histologic liver pathology. ANOVA testing showed that HU values of fibrosis, cirrhosis, as well as moderate and severe steatosis significantly differed from HU values of non-pathologic livers (Table 2). Overlapping of HU value ranges was observed between fibrosis, cirrhosis, as well as slight and moderate steatosis. Values below 30 HU and negative HU values were solely present in cases with severe steatosis (Fig. 2).

Liver hyperemia was observed in a total of 69 cases ($n = 29$ in non-pathologic livers, $n = 23$ in steatosis grade I, $n = 11$ in steatosis grade II, $n = 4$ in steatosis grade III, and $n = 1$ in fibrotic livers). ANOVA testing showed no significant differences between HU values of non-pathologic livers without hyperemia and non-pathologic livers with hyperemia ($p > 0.05$) as well as between steatosis grade I with hyperemia and steatosis grade I without hyperemia ($p > 0.05$). Case numbers of hyperemia in steatosis grade II and grade III as well as in fibrosis and cirrhosis were too low to allow for statistical analysis.

Table 1 Study group information

	Non-pathologic	Steatosis grade I	Steatosis grade II	Steatosis grade III	Cirrhosis	Fibrosis
<i>n</i>	64	61	37	23	19	10
Age	53.4	60.3	60.4	54.9	63.2	42
Sex (f/m)	38/25	19/43	11/26	11/12	6/13	5/5
PMI (d)	1.4	1.5	2	1.6	1.7	1.3

Sex, mean age, and mean PMI (time from death to CT scan) of defined liver groups

Cases with intoxication and metabolic derailment as cause of death did not exhibit histologic alterations other than steatosis, fibrosis, or cirrhosis.

The calculations for inter-observer error and intra-observer error (Table 3) showed that there was no relevant difference between two liver HU measurement series conducted by one and the same observer or two different observers.

Discussion

Liver steatosis, fibrosis, and cirrhosis are common diseases and thereby often found at autopsy as secondary diagnostic findings [24]. In unenhanced clinical CT, there are purely morphological traits by which liver steatosis and cirrhosis may be diagnosed. Such traits are based on visual organ changes such as size and shape of the liver and apparent image radiopacity and contrast changes [17–19, 25, 26]. In unenhanced clinical CT, severe liver steatosis may present as organ hypertrophy and noticeable hypo-density compared to surrounding organs such as the spleen [17–19]. In liver cirrhosis, the organ may appear with enlargement of the left lobe and caudate lobe, irregularity of the external contour of the left lobe and organ atrophy. Liver cirrhosis may also be accompanied by portal collaterals and ascites [25, 26]. In PMCT, no systematic studies exist that would confirm these morphologic signs for deceased persons. Nevertheless, there are few case reports that described the forenamed morphological criteria of cirrhosis and severe steatosis in PMCT in a short post mortem interval [27, 28]. However, those criteria are not obligatory findings or they may appear to be ambiguous. In such cases,

PMCT HU value measurements may be used as an additional tool for detection of unspecific liver pathology.

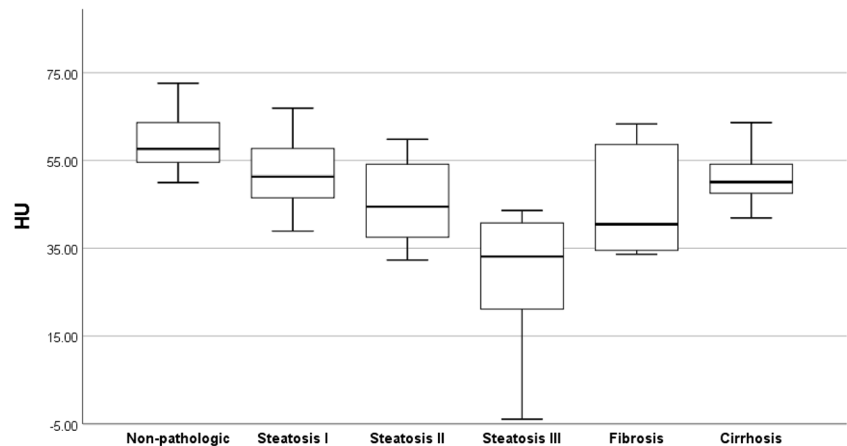
In the current PMCT study, HU values assessed for non-pathologic livers were in a range between 50 and 70 HU. Similar HU value ranges are known for non-pathologic livers in the living [5, 16–19]. To the best of our knowledge, there are no clinical studies that investigated unenhanced HU values of liver fibrosis or cirrhosis. Several clinical studies investigated HU values of liver steatosis in unenhanced clinical CT. In these studies, relevant liver steatosis was diagnosed at values below 40 HU [29, 30]. One clinical CT study correlated different histological grades of liver steatosis with liver HU values and found mean values of 59.1 HU for slight, 41.9 HU for moderate, and 25 HU for severe steatosis [15], which are similar to the post-mortem results of the present study. Hence, in a short post-mortem interval of few days, post-mortem phenomena such as biochemical degradation and diffusion processes as well as beginning putrefaction appear not to alter liver radiodensity. However, it is likely to assume that longer post-mortem intervals with advancing putrefaction will alter liver radiodensity due to gaseous tissue inclusion and tissue liquefaction. The results of the present PMCT study indicate that Hounsfield values beneath 50 HU may indicate liver pathology. However, in a range between 30 and 50 HU, the image reader may not be able to differentiate between moderate steatosis, fibrosis, or cirrhosis based only on HU measurements due to overlapping of HU values. This may be due to the fact that cirrhosis and fibrosis usually also contain relevant amounts of hepatocytes with fatty vacuoles as can be observed in the histology in Fig. 1b. Nevertheless, in cases where morphological PMCT criteria indicating liver pathology are ambiguous, HU measurements may strengthen radiologic

Table 2 ANOVA testing between non-pathologic livers and liver pathology

	Non-pathologic	Steatosis grade I	Steatosis grade II	Steatosis grade III	Fibrosis	Cirrhosis
Mean HU (SD)	58.32 (8.91)	52.91 (9.82)	45.7 (11.43)	32.44 (13.76)	44.7 (16.31)	50.59 (9.42)
ANOVA <i>p</i> value	/	0.07	0.03	0.001	0.02	0.04

Mean HU values and standard deviations of defined liver groups. ANOVA testing was performed between HU values of non-pathologic livers and groups with liver pathology

Fig. 2 HU values of non-pathologic livers and liver pathology. Boxplots depicting distribution of HU values (minimum, lower quartile, median, upper quartile, and maximum) of non-pathologic livers and liver pathology. Notice that least overlapping of HU values can be observed in severe liver steatosis



diagnosis of cirrhosis, fibrosis, or steatosis. Remarkably, PMCT values beneath 30 HU strongly indicate severe steatosis because fibrosis, cirrhosis, or moderate steatosis did not exhibited HU ranges less than 30 in our study.

Acute blood congestion did not significantly influence liver HU values of non-pathologic livers which may be explained by similar HU value ranges of post-mortem blood and non-pathologic liver tissue [10]. It can be assumed that in structural liver pathology with significantly lower tissue HU values, such as severe steatosis, blood congestion may influence HU values. However, case numbers of acute congested steatosis in the present study were too low to allow for valid statistical analysis to verify this thesis.

So far, only few applications for HU measurements in PMCT have been described in the literature [6, 8–10]. Liver HU measurements are relatively easy to perform on standard radiologic workstations and appear to be reproducible in a post-mortem approach. Some liver pathology such as steatosis and fibrosis usually affect the whole organ. Hence, to detect such pathology by means of HU measurements, it is less important where the measurement field is placed. However, focal liver pathology such as liver tumors may be regularly missed by untargeted HU liver measurements since they are usually hard to detect in unenhanced CT images.

Study limitations: In deceased bodies, the liver is usually the first organ that is affected by gas accumulations in liver

blood vessels due to putrefaction. Such putrefaction gas accumulations may appear even in shorter post-mortem intervals of only a few hours depending on body conditions and ambient temperatures at the time of death [31–33]. As putrefaction advances, the liver may appear with moderate to extensive emphysema in PMCT [21]. When placing ROIs for liver HU measurements in PMCT images, the image reader has to take care not to positioning ROIs in gas accumulations since this would falsify HU values and its interpretation. In advanced putrefied livers exhibiting grade II (moderate emphysema) and grade III (extensive emphysema) of the radiological alteration index from Egger et al. [21], HU measurements should not be performed due to tissue gas accumulations. In PMCT, liver HU measurements may also be affected by beam hardening effects due to the arms which are usually not lifted up but resting beside the torso. In the present study setup, we experienced that if beam hardening effects are indeed present, there usually are still liver areas left which are not affected and can be measured. In some cases, however, focal liver pathology may be overseen due to arm-related beam hardening effects. The CT beam energy applied was 130 kV and temperatures of corpses were not assessed prior to PMCT. It is known that HU values are dependent on beam energy [10, 11, 34, 35]. Hence, HU values presented in this study only account for beam energy of 130 kV. However, in unenhanced PMCT, usually beam energies between 110 and 130 kV are being used

Table 3 Intra- and inter-observer error

	Mean HU difference \pm SD	Min–max HU difference	<i>t</i> test <i>p</i> value
Intra-observer	2.2 \pm 1.7	0–3.1	0.093
Inter observer	2.8 \pm 2.1	0.5–8.2	0.062

Mean differences of HU values between two measurement series of one and the same observer (intra-observer) and two different observers (inter-observer) within randomly selected 20 cases of the study group (column two). Minimal and maximal differences of HU values between two measurement series are shown in column 3. *T* testing revealed there were no significant differences between inter-observer and intra-observer measurements series

for fresh corpses; and in a range of 20 kV, relevant changes of HU values are not to be expected [10, 11, 34]. Temperatures of fresh corpses scanned in PMCT usually range between 4 and 25 °C. According to Zech et al., relevant alterations of HU values are not to be expected within that temperature range in PMCT [10].

Conclusion

PMCT-unenhanced liver HU value measurements may be used as an additional method to detect unspecific liver-pathology. Liver HU values below 30 may specifically indicate severe steatosis.

Acknowledgements We would like to express our gratitude to our team of forensic pathologists and forensic technicians for their support with case handling.

Publisher's note Springer Nature remains neutral with regard to jurisdictional claims in published maps and institutional affiliations.

References

- Flach PM, Thali MJ, Germerott T (2014) Times have changed! Forensic radiology—a new challenge for radiology and forensic pathology. *AJR Am J Roentgenol* 202(4):W325–W334
- Lundström C, Persson A, Ross S, Ljung P, Lindholm S, Gyllensvärd F, Ynnerman A (2012) State-of-the-art of visualization in post-mortem imaging. *APMIS* 120(4):316–326
- Christe A, Flach P, Ross S, Spendlove D, Bolliger S, Vock P, Thali MJ (2010) Clinical radiology and postmortem imaging (Virtopsy) are not the same: specific and unspecific postmortem signs. *Leg Med (Tokyo)* 12(5):215–222
- Strandberg S, Wretling ML, Wredmark T, Shalabi A (2010) Reliability of computed tomography measurements in assessment of thigh muscle cross-sectional area and attenuation. *BMC Med Imaging*:10–18
- Pickhardt PJ, Park SH, Hahn L, Lee SG, Bae KT, Yu ES (2012) Specificity of unenhanced CT for non-invasive diagnosis of hepatic steatosis: implications for the investigation of the natural history of incidental steatosis. *Eur Radiol* 22(5):1075–1082
- Ruder TD, Thali Y, Schindera ST, Dalla Torre SA, Zech WD, Thali MJ, Ross S, Hatch GM (2012) How reliable are Hounsfield-unit measurements in forensic radiology? *Forensic Sci Int* 220(1–3):219–223
- Klop AC, Vester MEM, Colman KL, Ruijter JM, Van Rijn RR, Oostra RJ (2017) The effect of repeated freeze-thaw cycles on human muscle tissue visualized by postmortem computed tomography (PMCT). *Clin Anat* 30(6):799–804
- Schober D, Schwendener N, Zech WD, Jackowski C, Post-mortem CT (2017) Hounsfield unit profiles obtained in the lungs with respect to the cause of death assessment. *Int J Legal Med* 131(1):199–210
- Zech WD, Jackowski C, Schwendener N, Brenicova E, Schuster F, Lombardo P (2016) Postmortem CT versus forensic autopsy: frequent discrepancies of tracheobronchial content findings. *Int J Legal Med* 130(1):191–198
- Zech WD, Jackowski C, Buetikofer Y, Kara L (2014) Characterization and differentiation of body fluids, putrefaction fluid, and blood using Hounsfield unit in postmortem CT. *Int J Legal Med* 128(5):795–802
- Huda W, Slone R (2003) Review of radiologic physics, 3rd edn. Lippincott Williams & Wilkins, Philadelphia
- Allen BC, Barnhart H, Bashir M, Nieman C, Breault S, Jaffe TA (2012) Diagnostic accuracy of intra-abdominal fluid collection characterization in the era of multidetector computed tomography. *Am Surg* 78(2):185–189
- Bydder GM, Kreel L (1980) Attenuation values of fluid collections within the abdomen. *J Comput Assist Tomogr* 4(2):145–150
- Churchill RJ (1989) CT of intra-abdominal fluid collections. *Radiol Clin N Am* 27(4):653–666
- Kodama Y, Ng CS, Wu TT, Ayers GD, Curley SA, Abdalla EK, Vauthey JN, Chamsangavej C (2007) Comparison of CT methods for determining the fat content of the liver. *Am J Roentgenol* 188(5):1307–1312
- Hahn L, Reeder SB, Del Rio AM, Pickhardt PJ (2015) Longitudinal changes in liver fat content in asymptomatic adults: hepatic attenuation on unenhanced ct as an imaging biomarker for steatosis. *Am J Roentgenol* 205(6):1167–1172
- Zeb I, Li D, Nasir K, Katz R, Larijani VN, Budoff MJ (2012) Computed tomography scans in the evaluation of fatty liver disease in a population based study: the multi-ethnic study of atherosclerosis. *Acad Radiol* 19(7):811–818
- Hamer OW, Aguirre DA, Casola G, Lavine JE, Woenckhaus M, Sirlin CB (2006) Fatty liver: imaging patterns and pitfalls. *Radiographics* 26(6):1637–1653
- Boyce CJ, Pickhardt PJ, Kim DH, Taylor AJ, Winter TC, Bruce RJ, Lindstrom MJ, Hinshaw JL (2010) Hepatic steatosis (fatty liver disease) in asymptomatic adults identified by unenhanced low-dose CT. *Am J Roentgenol* 194(3):623–628
- Brogdon BG (2010) Brogdon's forensic radiology, 2nd edn. CRC Press, Boca Raton
- Egger C, Vaucher P, Doenz F, Palmiere C, Mangin P, Grabherr S (2012) Development and validation of a postmortem radiological alteration index: the RA-index. *Int J Legal Med* 126(4):559–566
- Recommendation no. R (99) 3 of the Committee of Ministers to member states on the harmonization of medico-legal autopsy rules (2000) *Forensic Sci Int* 111(1–3):5–58
- Brunt EM (2005) Pathology of nonalcoholic steatohepatitis. *Hepatology* 41(2):68–71
- Kumar V, Abbas AK, Aster JC (eds) (2015) Robbins & Cotran: pathologic basis of disease. 9th ed. Elsevier Saunders, Philadelphia
- Zeitoun D, Brancatelli G, Colombat M, Federle MP, Valla D, Wu T, Degott C, Vilgrain V (2004) Congenital hepatic fibrosis: CT findings in 18 adults. *Radiology* 231(1):109–116
- Brancatelli G, Baron RL, Peterson MS, Marsh W (2003) Helical CT screening for hepatocellular carcinoma in patients with cirrhosis: frequency and causes of false-positive interpretation. *AJR Am J Roentgenol* 180(4):1007–1014
- Bott E, O'Donnell C, Burke M (2013) Post mortem CT demonstration of hemoperitoneum caused by rupture of a paraumbilical vein into a paraumbilical hernia in a man with liver cirrhosis and portal hypertension. *Forensic Sci Med Pathol* 9(1):77–81
- Usui A, Kawasumi Y, Hosokai Y, Saito H, Igari Y, Funayama M (2013) Fatal intra-abdominal hemorrhage as a result of avulsion of the gallbladder: a postmortem case report. *Acta Radiol Short Rep* 2(2):2047981613482898
- Wells MM, Li Z, Addeman B, McKenzie CA, Mujoomdar A, Beaton M, Bird J (2016) Computed tomography measurement of hepatic steatosis: prevalence of hepatic steatosis in a Canadian population. *Can J Gastroenterol Hepatol* 2016:4930987
- Lawrence DA, Oliva IB, Israel GM (2012) Detection of hepatic steatosis on contrast-enhanced CT images: diagnostic accuracy of identification of areas of presumed focal fatty sparing. *AJR Am J Roentgenol* 199(1):44–47

31. Yokota H, Yamamoto S, Horikoshi T, Shimofusa R, Ito H (2009) What is the origin of intravascular gas on postmortem computed tomography? *Leg Med (Tokyo)* 11(Suppl 1):S252–S255
32. Jackowski C, Sonnenschein M, Thali MJ, Aghayev E, Yen K, Dirnhofer R, Vock P (2007) Intrahepatic gas at postmortem computed tomography: forensic experience as a potential guide for in vivo trauma imaging. *J Trauma* 62(4):979–988
33. Gebhart FT, Brogdon BG, Zech WD, Thali MJ, Germerott T (2012) Gas at postmortem computed tomography—an evaluation of 73 non-putrefied trauma and non-trauma cases. *Forensic Sci Int* 222(1–3):162–169
34. Schmitt WG (1986) Energy dependence of Hounsfield numbers. *Röfo* 145(2):221–223
35. Bydder GM, Kreel L (1979) The temperature dependence of computed tomography attenuation values. *J Comput Assist Tomogr* 3(4):506–510